

Morphological plasticity of bacteria—Open questions

Jie-Pan Shen^{1,2,3} and Chia-Fu Chou^{3,4,5,a)}

¹*Department of Engineering and System Science, National Tsing Hua University, Hsinchu 30013, Taiwan*

²*Nano Science and Technology Program, Taiwan International Graduate Program, Academia Sinica, Taipei 11529, Taiwan and National Tsing Hua University, Hsinchu 30013, Taiwan*

³*Institute of Physics, Academia Sinica, Taipei 11529, Taiwan*

⁴*Genomics Research Center, Academia Sinica, Taipei 11529, Taiwan*

⁵*Research Centre for Applied Sciences, Academia Sinica, Taipei 11529, Taiwan*

(Received 1 February 2016; accepted 23 May 2016; published online 10 June 2016)

Morphological plasticity of bacteria is a cryptic phenomenon, by which bacteria acquire adaptive benefits for coping with changing environments. Some environmental cues were identified to induce morphological plasticity, but the underlying molecular mechanisms remain largely unknown. Physical and chemical factors causing morphological changes in bacteria have been investigated and mostly associated with potential pathways linked to the cell wall synthetic machinery. These include starvation, oxidative stresses, predation effectors, antimicrobial agents, temperature stresses, osmotic shock, and mechanical constraints. In an extreme scenario of morphological plasticity, bacteria can be induced to be shapeshifters when the cell walls are defective or deficient. They follow distinct developmental pathways and transform into assorted morphological variants, and most of them would eventually revert to typical cell morphology. It is suggested that phenotypic heterogeneity might play a functional role in the development of morphological diversity and/or plasticity within an isogenic population. Accordingly, phenotypic heterogeneity and inherited morphological plasticity are found to be survival strategies adopted by bacteria in response to environmental stresses. Here, microfluidic and nanofabrication technology is considered to provide versatile solutions to induce morphological plasticity, sort and isolate morphological variants, and perform single-cell analysis including transcriptional and epigenetic profiling. Questions such as how morphogenesis network is modulated or rewired (if epigenetic controls of cell morphogenesis apply) to induce bacterial morphological plasticity could be resolved with the aid of micro-nanofluidic platforms and optimization algorithms, such as feedback system control. *Published by AIP Publishing.* [<http://dx.doi.org/10.1063/1.4953660>]

INTRODUCTION

Bacterial cell morphology is essentially conferred by the generation of peptidoglycan (PG) exoskeleton or murein sacculus, which is typically known as the cell wall. How the cell wall is generated and maintained is a critical question to address in bacterial morphogenesis. The cell wall is a mesh-like structure and composed of peptidoglycan strands that are crosslinked by pentapeptide bridges connected to the repeating subunits of N-acetylmuramic acid and N-acetylglucosamine.¹ This hard-shell enclosure in bacteria is rigid enough to retain the shape consistency, while flexible to allow dynamic modifications by a variety of PG assembly enzymes and cell morphogenesis proteins.¹ The indication that active modifications of PG structures are spatiotemporally modulated by an array of enzymes and regulators in morphogenesis reflects the

^{a)} Author to whom correspondence should be addressed. Electronic mail: cfchou@phys.sinica.edu.tw

capability of bacteria to adapt certain morphologies and as such to gain advantages in coping with stressful environmental contexts and unfavorable niches. Whereas, unlike the impression from our macroscopic experiences that certain morphologies confer specific advantages for better fitness, different bacterial species may take different adaptive strategies to gain advantages in a given environment. Therefore, multiple morphologies can be found for different bacterial species adapting to the same environment. Depending on selective pressures, physical constraints, and patterns of cell growth and division, bacterial morphology is widely diverse even in closely related genera but can be highly conserved across distant taxa.² Other factors such as nutrient availability, sessility and dispersal strategies, motility requirements, and predation pressures may also contribute to bacterial morphologies such as to gain advantages in response to different environmental cues.³ Notably, evolutionary changes in bacterial morphology can even occur in some bacterial species exhibiting pleomorphic life cycle. Namely, a single population of bacteria exhibit morphological variations to promote their survival capability and altered mode of reproduction as opposing to environmental shifts. This phenomenon is known as bacterial morphological plasticity and considered as a survival strategy by associating morphological changes as a natural part of their life cycle.⁴ For some bacteria in their natural habitats, such as *Caulobacter crescentus* in nutrient-limited freshwater⁵ and uropathogenic *Escherichia coli* (UPEC) in mammalian urinary tract,⁶ morphological plasticity in these bacteria plays a pivotal role in promoting survival advantage against extreme environments.

Perhaps, the most intriguing but less noticeable cell type associated with morphological plasticity are cell wall deficient or defective bacteria (CWDB), or L-forms. CWDB can be generated spontaneously or by induction in various bacterial species as part or all of their cell wall are deprived.^{7,8} It is a realistic survival strategy exploited to protect bacteria against cell wall targeting antibiotics and the immune system.⁹ The proliferation of CWDB is independent of the normal essential cell division machinery but involves a mechanism of membrane dynamics such as tubulation or blebbing.¹⁰ Therefore, it is suggested that the unusual mode of proliferation provides a model for the primitive progenitor of bacteria and the origins of life.¹¹ Moreover, CWDB can develop a variety of intermediate states associated with diverse cell morphologies on the pathways reverting to original morphology.^{11,12} It is unclear that these morphological variants are transitional or due to environmental stresses, but specific morphological variants have been reported to link to stress response/accessory envelope proteins in lysozyme-induced CWDB.¹³ Because the expression of these proteins are known to be induced by environmental stresses such as starvation or outer membranes damage, the development of phenotypical plasticity in CWDB is implicated to enable diversified interactions between assorted reverting pathways and environmental contexts in the population level. Further, the simple geometric effect to retain surface to volume ratio¹⁰ and the requirement of peculiar genes for membrane synthesis and integrity^{13,14} have been identified to ensure the proliferation and survival of CWDB morphological variants. It is apparent that the morphological plasticity of CWDB provides a plausible survival strategy for severely injured bacteria coping with environmental stresses.

Recently, artificially obstructed synthesis of cell wall in bacteria confronting physical constrictions was shown to alter bacterial morphologies or induce morphological variation.^{15–17} *E. coli* can be molded to form spiral shape and show altered motility.¹⁶ Squashed *E. coli* and *Bacillus subtilis* cells sculpted by nanofluidic confinement exhibit morphological aberrancy due to derailed PG assembly under the strong confinement.¹⁵ Owing to the act of nucleoid occlusion, these aberrant cells can perform symmetric cell division in the restricted space with dimension about one half of typical cell diameter at least in one dimension. These aberrant bacteria can revert to original short rods after serial cell divisions in a stress-free environment. It is known for some bacteria such as *C. crescentus*, a prolonged culture can induce morphological plasticity.⁵ Under the physical constraints of periodic micro-nanofluidic junctions, morphological plasticity in *E. coli* cells can be induced in a prolonged culture and the developed morphological variants resemble multiple cell types discovered in CWDB.¹⁷ These examples suggest at least for *E. coli*, strongly physical intervention of PG assembly to distort cell wall synthesis can induce morphological plasticity in a prolonged culture. In this review, we will discuss briefly

the current status of bacterial morphogenesis and the sources of these morphological changes. Further, we will pinpoint some open questions and the future directions to study the morphological plasticity of bacteria, particularly using physical constraints by artificial micro- and nano-fluidic structures.

BACTERIAL MORPHOGENESIS

Evolutionary biologists, based on phylogenetic analysis, inferred that the last common ancestor of bacteria could be rod shaped.¹⁸ It is intriguing how other bacteria shapes are generated and whether it is possible to generate other bacterial shapes from rod-shaped bacteria via the induction of CWDB, i.e., acquiring the capability of primitive progenitor of bacteria in cellular organization.¹¹ Since the cell shapes in distinct bacterial species, ranging from classic spheres, rods, and spirals to unconventional squares, coils, chains, stars, and bifidity, are so diversified, one may wonder what genetic origins and molecular mechanisms underlie bacterial cell shape generation and the transition leading to morphological variation. However, even for simple sphere, rod, and crescent shapes, the solutions to generate the same shape might be varied among different species. Conceptually, the bacterial morphogenesis is steered through the modulations of PG assembly, which are carried out by assorted patterns of bacterial growth and cytokinesis under the normal physiology of most bacterial species.¹⁹ First, bacterial growth can be modulated by the elongasome machinery that distributes PG synthesis either uniformly along cell body (dispersed and preseptal growth) or spatially upon one or multiple restricted zones (zonal growth).²⁰ Next, cytokinesis is partially facilitated by PG synthesis inwards that is directly or indirectly modulated by the divisome machinery.²¹ In most rod-shaped bacteria such as *E. coli* and *B. subtilis*, the elongasome is directed by actin homolog MreB and the divisome governed by the assembly of tubulin homolog FtsZ.^{12,19} Reduction of MreB or FtsZ expression level in *E. coli* can generate round or filamentous cells.⁴

Apart from spatial patterns, the temporal modulations of PG assembly directed by the elongasome and divisome machineries together give rise to six types of representatives in cell shape generation.¹⁹ Despite the requirement of active FtsZ-directed sidewall synthesis and constriction in the cell division of *E. coli*, both *B. subtilis* and *E. coli* generate rod-shaped cells by dispersed growth via the MreB-mediated elongasome machinery, then following preseptal growth via FtsZ-dependent septum synthesis during cytokinesis. Alternatively, the MreB-mediated dispersed growth in *C. crescentus* is slower and FtsZ-directed sidewall synthesis is less active in one side of cell body for the inhibition of crescentins such as to generate curved rods by following the constriction without the need of septum formation. For those bacterial species lacking MreB, *Streptococcus pneumoniae* simultaneously synthesize the septum and FtsZ-directed sidewall to generate ovococoids, while *Streptococcus aureus* only synthesize the septum to generate cocci. At last, *Corynebacterium glutamicum* also lacks MreB and exploits zonal growth at both cell poles by DivIVA to elongate cell body. Following the zonal growth, *C. glutamicum* synthesize the septum to generate rod-shaped daughter cells.

THE SOURCE OF BACTERIAL MORPHOLOGICAL CHANGES

While fascinating in bacterial morphological plasticity induced by distinct environmental contexts, limited clues and evidences are available to show the definite linkage between the environmental inductions and the molecular pathways that directly or indirectly modulate the PG assembly in the transformation of bacterial morphology. Some environmental cues such as innate immune effectors, protistan predation, quorum-sensing molecules, and antimicrobial agents are suggested to induce bacterial morphological plasticity.⁴ Whereas, the linkage of these environmental inductions to bacterial morphological changes via the modulation of PG assembly is not straightforward. For example, the transformation of UPEC²² and *Mycobacterium tuberculosis*²³ into filamentous bacteria is likely caused by the divisome inhibition through upregulation of the SOS response (*sulA*, *recA*, and *lexA*) and induced by phagocytic production of reactive oxygen species (ROS). Further, in another extreme case as cell wall is even partially lost, the generation of morphological variants during the CWDB development especially

requires proteins unrelated to the PG assembly for *de novo* generation of cell wall, such as the stress response/accessory envelope proteins¹³ and excess membrane synthesis.¹⁰ Interestingly, the process for morphological reversion from CWDB to their typical morphology still somewhat exploits the guidance of classic cytoskeletal systems.¹² The environmental cues to generate CWDB and their morphological variants are much shared with those identified to induce morphological plasticity in some bacterial species. Despite being elusive, the pathways associated with the modulation of PG assembly may be critical links to trigger the transformation of morphological changes in stressed bacteria. Here, we take *E. coli* as the major examples of morphological plasticity to discuss the source of bacterial morphological changes and the plausible linkage to the modulatory pathways of PG assembly.

- (1) *Starvation*: Nutrition depletion for bacteria is the most commonly encountered environmental stress that causes physiological changes to survive the fasting adversity. In particular, the carbon starvation might impact the modulation of PG synthesis. Apart from the altered metabolism, morphological change is also an apparent signature for starving bacteria. Most bacteria do not commonly grow in planktonic state but form a differentiated multicellular community, or biofilm, adhering to solid surface in their natural habitats. Huge variation of nutrient availability, oxygen concentration, and pH are found at different locations within bacterial biofilm. Therefore, such disparate microenvironments confer diversified physiology of sessile cells embedded within different niches of bacterial biofilm.²⁴ In *E. coli* macrocolony biofilms, three-dimensional structures (Figs. 1(a)–1(d)) emerge by the interplay of heterogeneous gene expression and differential environmental signals, as well as depend on self-producing extracellular matrix components such as amyloid curli fibers (Figs. 1(d)–1(e)) and cellulose (Figs. 1(b)–1(c) and 1(e)–1(h)).²⁵ The two-layer biofilm architecture (Figs. 1(a), 1(b), and 1(e)) facilitates the nutrient supply from the attached agar surface and induces morphological changes at cellular level depending on nutrient availability. In the nutrient-rich zones (green rectangle in Figs. 1(a) and 1(b) and enlarged views indicated by white inlets in Figs. 1(f) and 1(g)), elongated rod-shaped bacteria were found to be enmeshed by their flagella (yellow arrow in Fig. 1(b)), whereas in the nutrient-depleting zones (cyan rectangle in Figs. 1(a) and 1(c)) and enlarged views indicated by red inlets (Figs. 1(f) and 1(g)), starving bacteria lacking flagella

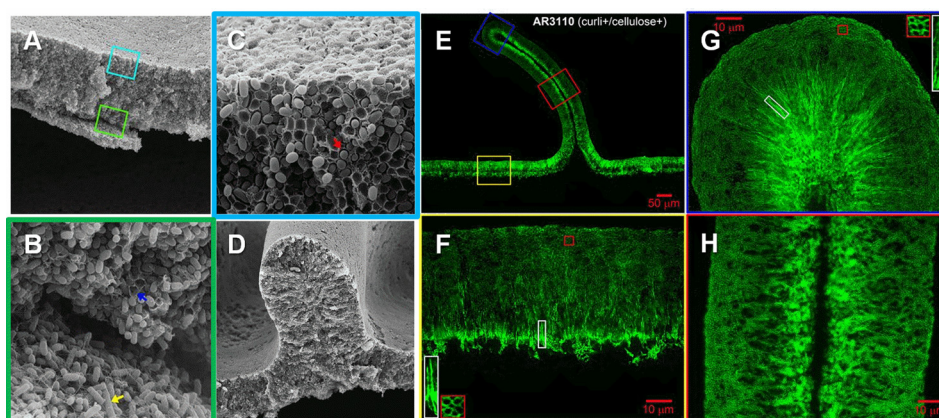


FIG. 1. Spatial arrangement of cellulose, curli and flagella, and cell morphology in the context of the two-layer *E. coli* AR3110 biofilm architecture. Low magnification SEM image of AR3110 biofilm cross-section at a flat area (a) and a small ridge (d) is shown and color boxes images (b and c) at 12000 \times magnification correspond to the color-boxed regions indicated in (a). Blue and yellow arrows in (b) indicate cells in contact with sheet-like cellulose structure at the base of upper layer and elongated rod-shaped cells enmeshed by their flagella in the lower layer, respectively. A red arrow in (c) indicates starving ovoid cells encapsulated by sheet-like cellulose structure in the upper layer. Panels (e)–(h) show differential distribution of cellulose and amyloid curli that exhibit specific spatial arrangement in AR3110 biofilm. Low magnification image in (e) shows amyloid staining thioflavin S (TS) fluorescence in an AR3110 biofilm cross-section. Enlarged views of TS fluorescence pattern in respective color-boxed images (f–h) correspond to the color-boxed regions in (e). The insets (f and g) specify spatial arrangement of amyloid curli fibers in respective color-boxed regions. Reprinted with permission from D. O. Serra *et al.*, J. Bacteriol. **195**, 5540 (2013). Copyright 2013 American Society for Microbiology.²⁵

were encapsulated in sheet-like and filamentous cellulose matrix allocated and exhibited ovoid-shaped (red arrow in Fig. 1(c)).

- (2) *Oxidative stress: Salmonella Typhimurium* as an intracellular pathogen has been found in macrophages to exhibit filamentous cell type in response to phagocytic effectors such as ROS that correlate to upregulation of the SOS response.²⁶ ROS can cause DNA damage in bacteria and as such trigger the SOS response that further antagonizes the polymerization of FtsZ to induce filamentous bacteria.⁴ The divisome inhibition is also known to prevent the preseptal elongation directed by FtsZ assembly and thus interfere the PG assembly in the septal zone.¹ The morphological change induced by oxidative stress has been widely observed in multiple pathogenic bacteria. In particular, the emergence of UPEC pleomorphism represents a typical example of bacterial morphological plasticity that serves as a survival strategy to escape killing from the innate immune system and facilitate pathogenesis in context with morphological changes during different developmental stages of urinary tract infection (Fig. 2(a)).⁶ When UPEC attach to the umbrella cells lining the urothelium surface, they hijack the cytoskeletal

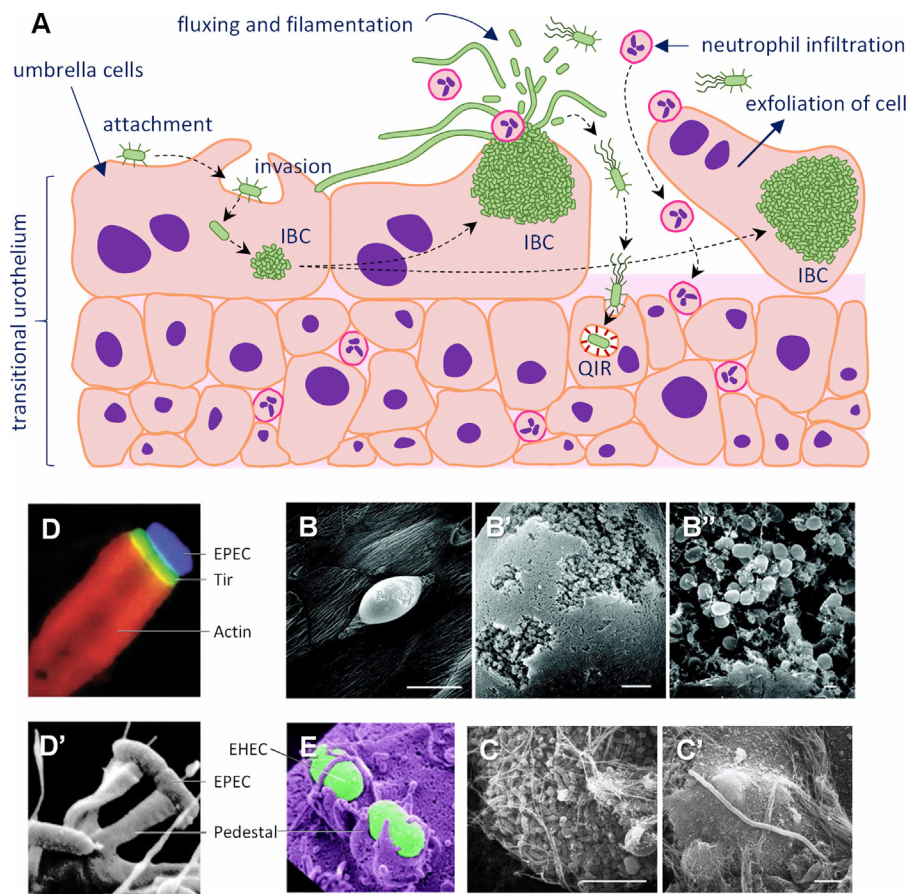


FIG. 2. (a-c') Morphological changes of uropathogenic *E. coli* (UPEC), (d-d') enteropathogenic *E. coli* (EPEC), and (e) enterohemorrhagic *E. coli* (EHEC). See texts for details about the pathogenic cascade of UPEC infection and the associated morphological changes (a). Modified with permission from M. A. Croxen and B. B. Finlay, Nat. Rev. Microbiol. 8, 26 (2010). Copyright 2010 Macmillan Ltd. (b-b'') SEM images of a pod on the surface of a mouse bladder infected with UPEC for 24 h show large intracellular bacterial communities (IBC) inside pods. Scale bars: 50 μm (b), 5 μm (b'), and 0.5 μm (b''). Reprinted with permission from G. G. Anderson *et al.*, Science 301, 105 (2003). Copyright 2003 American Association for the Advancement of Science. (c-c') SEM images of IBC (c) and long filamentous cells. (c-c') Scale bars: 5 μm . Reprinted with permission from D. A. Rosen *et al.*, PLoS Med. 4, e329 (2007).³⁴ Copyright 2007 Author(s), licensed under a Creative Commons Attribution License. Fluorescent (d) and SEM (d') images show the remodeled cytoskeletal structures and embedded EPEC on the actin-rich pedestal via Tir effector. Reprinted with permission from R. D. Hayward *et al.*, Nat. Rev. Microbiol. 4, 358 (2006). Copyright 2006 Macmillan Ltd.]. (e) Color-coded SEM image of actin-rich pedestal (purple) is rendered by EHEC (green). Reprinted with permission from S. Bhatt *et al.*, Trends Microbiol. 19, 217 (2011). Copyright 2011 Elsevier Ltd.³⁵

system of the host cells to engulf themselves and then multiply to form bacterial biofilms known as intracellular bacterial communities (IBC). Some IBC advance into matured biofilms and create pod-like bulges on the surface of infected cells, eventually leading to cell exfoliation (Figs. 2(b) and 2(b'')). Alternatively, during IBC maturation, some subpopulation of IBC cease cell division and transform into *SulA*-mediated filamentous bacteria.²² The filamentous bacteria, together with the late stage rod-shaped IBC subpopulation, may flux out of the pods (Figs. 2(c) and 2(c')) and take advantages to escape from neutrophil killing. They may either attack other naive epithelial cells or exit the host cell with urine flow. Moreover, the release of endotoxin lipopolysaccharides (LPS) can stimulate Toll-like receptor 4 (TLR-4) that recruits neutrophils to eliminate bacteria. Filamentous morphology increases the number of adhesins for stronger attachment on the host cells and as such resist phagocytosis by phagocytic cells. Once exfoliation of superficial umbrella cells occurs, UPEC can invade the deeper cell layer of urothelium. These invading UPEC may associate with actin fibers to reside in the low pH endosome-like compartment of the host cell and thus become quiescent intracellular reservoirs (QIR; Fig. 2(a)), which is believed to involve in UPEC persistence and resurgence.²⁷ Apparently, QIR formation can help UPEC escape from neutrophil phagocytic killing and avoid oxidative stress, yet it is unclear what induces intracellular UPEC generate endosome-like cell morphology.

- (3) *Predation effectors*: Under the aquatic microbial network, phagotrophic flagellates and heterotrophic nanoflagellates are the major bacterivory predators in a size less than 10 μm . It is suggested by the bimodal effect that bacterial cells in an intermediate size are much easily grazed by the grazing protists.²⁸ Interestingly, formation of filamentous and curved-shaped *Flectobacillus spp.* has been experimentally induced when they directly confronted with flagellate grazer *Orchomonas spp.* or simply responded to grazer excretory effectors within a chemostat.²⁹ Although the molecular basis of grazer excretory effectors remains entirely unknown, it is very likely that their working mechanism might involve the described pathway of divisome inhibition. In addition to morphological plasticity, other survival strategies such as motility patterns, biofilm formation, toxin release, and quorum sensing have been evolved in bacteria to circumvent the predation from protistan predation pressure.²⁸ It is not surprised that these survival strategies are widely adopted by pathogenic bacteria to circumvent immune surveillance in pathogenesis.⁴ As described in the earlier example, UPEC transform into filamentous bacteria in respond to phagocytic effectors ROS. Moreover, UPEC also generate the actin-gated QIR and hibernate inside the host cell for later resurgence. The capability to hijack the cytoskeletal system of host cell confers pathogenic bacteria gaining better survival and dispersal advantages to cope with immune effectors. Unlike UPEC, enteropathogenic and enterohemorrhagic *E. coli* (EPEC and EHEC) can remodel the cell morphology of infected enterocytes, rather than bacteria *per se*, and have themselves intimately embedded in the remodeled cellular structure called actin-rich pedestal by reorganizing the actin machinery of host cell^{30,31} (Figs. 2(d) and 2(e)). Exceptionally, actin-rich pedestals induced by EPEC and EHEC are not static but propel the bacteria on the apical surface of enterocytes at the moving speed up to 4.2 μm per minute.³² Such an actin-dependent cellular structure for intimate attachment and motility pattern helps EPEC and EHEC avoid immune surveillance and likely facilitates the subversion of professional phagocytes by blocking opsono-phagocytosis via the action of specific effectors.³³
- (4) *Antimicrobial agents*: Many antimicrobial agents, including antibiotics, antimicrobial peptides and degradative enzymes, target cell wall, cell membranes, nucleic acids, and proteins related to chromosome replication. Some β -lactam antibiotics target the active site of penicillin-binding proteins (PBPs). L-form induction medium containing up to 6 mg/ml penicillin G was reported to induce *E. coli* spheroids on soft agar⁸ (Figs. 3(a) and 3(b)). Their mode of action is to block the transpeptidation step of PG assembly, which is normally catalyzed by PBPs for the crosslinking between nascent PG layers.³⁶ Whereas, many clinic samples retrieved from the patients treated with β -lactams displayed filamentous bacteria. The obstructed PG assembly caused by β -lactams in *E. coli* has been shown to inactivate *ftsI* gene product PBP-3 by eliciting the SOS response (*recA* and *lexA*) through the DpiBA two-component signal

transduction system. The activation of DpiBA signaling due to β -lactams exposure enables the effector DpiA not only altering transcription of target genes but also leading to competitive blocking of the replication origin of *E. coli* chromosome, thereby inhibiting cell division.³⁷ In particular, high concentration of β -lactams, amino acids (glycine and phenylalanine agents), and peptidase and lytic enzymes that degrade the cell wall can induce almost all known bacterial species into CWDB and the following morphological variants.⁹ These examples clearly indicate the linkage of morphological changes to the modulatory pathways of PG assembly when bacteria respond to antimicrobial agents.

- (5) *Temperature stresses*: Bacteria are perhaps the most adaptive organisms on the earth. They can be found in the boiling water of hot spring, as well as in the supercooled water of subglacial rift lakes underneath Antarctic ice shell around 500 m below sea level. But for most bacterial species, they do grow within acceptable temperature window. It can be imagined the structures of cell membranes and cell wall would be seriously damaged under the extreme temperature such as freezing and boiling points. However, transition of bacteria into pleomorphic L-forms, i.e., CWDB, has been considered as a potential mechanism for bacterial survival under unfavorable conditions.⁹ Intriguingly, high cell density population of *E. coli* has been undertaken lethal treatment of boiling or autoclaving such as to induce the transformation of surviving bacteria CWDB. These bacteria proliferated on soft agar medium by likely exploiting membrane dynamics such as budding process as shown in starving *E. coli* CWDB (Fig. 3(c)) and later developed toward distinct morphological variants (Figs. 3(d) and 3(e)).³⁸ The heat-induced CWDB experienced a variety of morphological changes and then fully reverted to typical rod-shaped *E. coli* after 5 passages at 24 h intervals.
- (6) *Osmotic shock*: Lysozyme is also an antimicrobial agent targeting bacterial cell wall and widely presents at high concentrations in body fluids such as tears, saliva, stomach juice, milk, and respiratory mucosa. The breakdown of cell wall integrity due to lysozyme attack would cause bacteria bursting out under their own internal osmotic pressure. Accordingly, lysozyme has been used in the generation of CWDB in context with spheroplasts from gram-negative

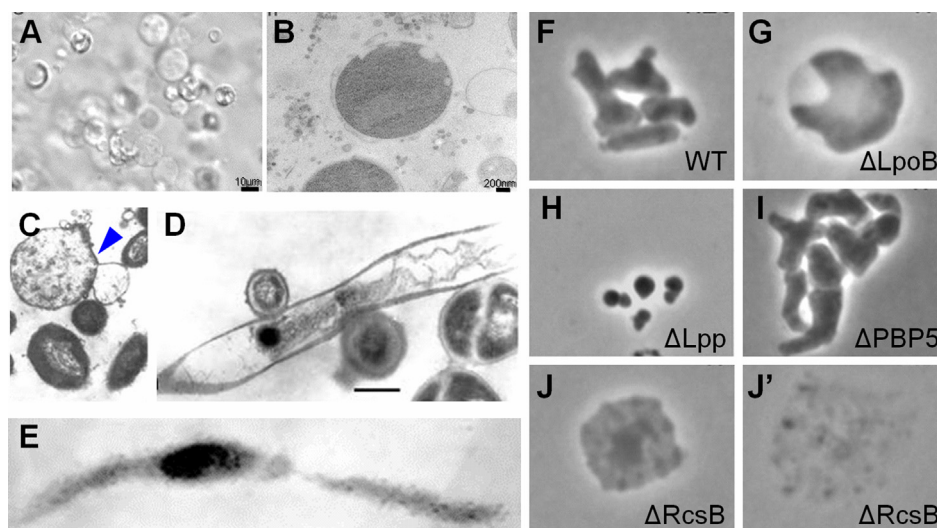


FIG. 3. Morphological variants derived from *E. coli* CWDB. SEM (a) and TEM (b) images show *E. coli* spheroids induced by high concentration of penicillin G on soft agar. Cell diameter ranges between 2 and 30 μm . Reprinted with permission from W. A. Glover *et al.*, PLoS One 4, e7316 (2009). Copyright 2009 Author(s), licensed under a Creative Commons Attribution License. A prolonged culture (14 days) of *E. coli* under starvation can induce transformation into CWDB on soft agar as shown in TEM image (c). A blue arrow in (c) indicates cell proliferation by budding. *E. coli* CWDB can be also induced to develop various morphologies (d and e) on soft agar after heat treatment by either autoclaving or boiling. Scale bar: 200 nm for (c-e). Reprinted with permission from N. Markova *et al.*, Int. J. Biol. Sci. 6, 303 (2010). Copyright 2010 Ivyspring Intl. Panels (f)-(j') show assorted morphological variants of lysozyme-induced *E. coli* CWDB. In each image, genetic alteration is indicated and WT stands for wild type *E. coli*. The size of microcolony is about 5-10 μm . Reprinted with permission from D. K. Ranjit and K. D. Young, J. Bacteriol. 195, 2452 (2013). Copyright 2013 American Society for Microbiology.

bacteria¹³ or protoplasts from gram-positive bacteria.⁹ These CWDB proceeded a series of cell division and reverted to rod-shaped bacteria. Such a morphological reversion from lysozyme-induced *E. coli* CWDB, together with mutagenesis of stress response system and accessory proteins, generated plethora morphological variants (Figs. 3(f)–3(j')) and helped identification of auxiliary mechanisms that are required to supplement the classic FtsZ- and MreB-directed cell wall synthesis.¹³ Here, one stress response system (Rcs) and three accessory envelop proteins (PBP1B, LpoB, and Lpp) are essential in *E. coli* for morphological reversion without the aid of previously completed PG template.

- (7) *Mechanical constraints*: MreB proteins appear to be the master geometric regulators apt to organize into extended filaments to modulate the PG synthesis and turnover through interactions with assorted components of cell wall synthetic machinery.³⁹ MreB filaments are suggested to be recruited at membrane sites with favored curvatures such that termination of filament extension at sites of incompatible geometry would cause the predominance of short MreB filaments when morphological aberrancy happened on a cell. Further, MreB filaments recruit multiple PG synthetic complexes to insert new PG stands and direct the synthetic complexes moving along the filaments. The motions are believed to drive processive movements of MreB filaments in the same direction. Such movements disappear when bacteria transform into lysozyme-induced CWDB.⁴⁰ It is therefore implicated that bacterial morphological changes may affect MreB filament dynamics and as such cell wall synthetic machinery is modulated via the guidance of MreB filament dynamics. Eventually, the interactions among bacterial morphological changes, MreB filament dynamics, and cell wall synthetic machinery would correct morphological aberrancy by attaching MreB filaments to sites of negative cell curvature such as to direct PG synthesis toward the reversion into typical bacterial morphology.⁴⁰ Accordingly, strong perturbation of bacterial morphology as they grow in submicron environment^{15,17} could prevent MreB filament extension and cease the movement of MreB filaments owing to the large area of flat cell membranes confined by the submicron fluidic chamber. Instead, short MreB filament is thought to attach to the negatively curved peripherals of squashed bacteria, by which bacteria undergo irregular cell growth in radial direction depending on the surrounding cells arranged by the interaction between bacterial population and physical confinement.

Therefore, the guidance of cell wall synthetic machinery by MreB filament dynamics for bacteria under strong confinement might be missing, leaving morphogenesis steered by FtsZ-directed PG synthesis and shapeshifting membrane dynamics. Strong submicron confinement contributes to the deformed and perhaps defective cell wall of squashed bacteria, by which modulations of cell wall synthesis were altered to induce the transformation leading to CWDB. It is not surprised these bacteria underwent morphological reversion after a series of cell divisions once they evaded from mechanical constraints. Herein, plethora morphological variants of *E. coli* cells (Fig. 4) were observed on the development of morphological reversion after a prolonged culture under the mechanical constraints of periodic micro-nanofluidic junctions.¹⁷ While intriguingly, these morphological variants are similar to those observed in

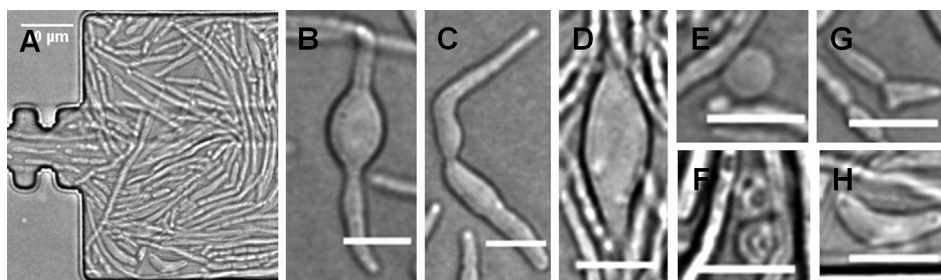


FIG. 4. (a-h) Bright-field images exhibit plethora morphological variants of *E. coli* that are induced by mechanical constraints.¹⁷ The morphological variants shown here were developed 3 h after bacteria were released into stress-free environment. Scale bars: (a) 10 μm ; others: 5 μm .

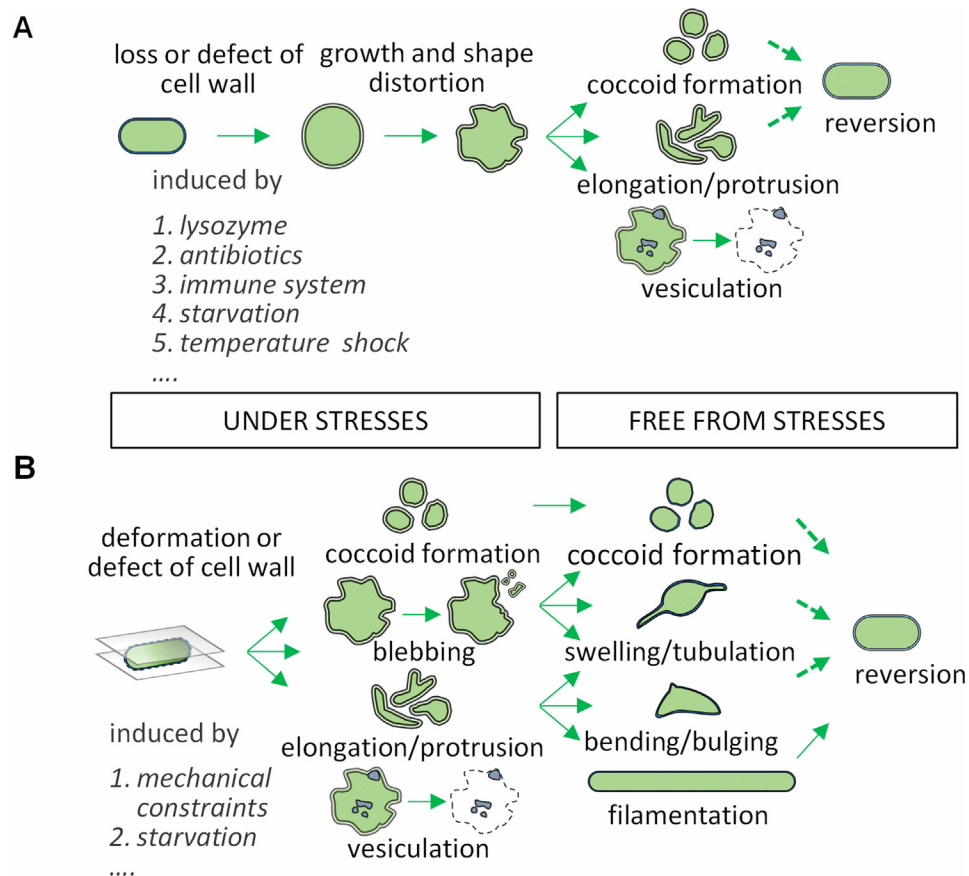


FIG. 5. A schematic comparison of morphological development and reversion based on (a) lysozyme-induced CWDB and (b) mechanically induced morphological variants of *E. coli*. Different sources that induce similar morphological changes and various types of cell morphologies are described in the texts and also indicated in respective cases.

lysozyme-induced spheroplasts (Figs. 3(f)–3(j') and 5(a)), except the morphological variants induced by lysozyme were partially conferred by the genetic deficiency of specific stress response/accessory/envelop proteins.¹³ In contrast to the alterations in genetic inheritance, it is suspected that reprogramming of morphogenesis network by differential gene expression and/or epigenetic controls is activated in mechanically induced morphological variants in complex with inactive MreB filament dynamics to further cell heterogeneity in stressed population for coping with the mechanical adversity. The stressed bacteria might undergo rounding, blebbing, elongation, protrusion, and vesiculation (Fig. 5(b)), some of which likely involve cell proliferation in the absence of the functional elongasome and/or divisome.¹¹ Once evading from strong confinement, the cell lineages of distinct morphological variants might regain the functional elongasome/divisome and proceed morphological reversion by advancing into different developmental pathways with featured morphogenesis processes, including coccoid formation, swelling and tabulation, bending and bulging, and mostly filamentation (Fig. 5(b)).

Why morphological plasticity?

Morphological plasticity may be beneficial to bacterial adaptation in changing environments. Nevertheless, there seems no consensus pathway to induce bacterial morphological plasticity. Also, the exact mechanism underlying the development of bacterial morphology in response to specific environmental contexts remains largely unknown. As described above, some environmental cues are suggested to induce bacterial morphological plasticity,⁴ yet the transition leading to morphological changes for bacteria may not be induced by only one

source. For example, *Proteus mirabilis* is an opportunistic urinary pathogen that switches cell morphology between short rods (swimmers) and elongated filamentous cells (swarmers). When *P. mirabilis* sense high quorum level, they initiate the differential gene expressions leading to cell filamentation and as such to facilitate swarming motility in response to flagellar contact with solid surface. This morphological change enhances their invasion to the host cells by the augmented numbers of adhesins, protects bacteria from phagocytosis by the host immune response, and upregulates the expression of metalloprotease that degrades mammalian antibacterial peptides.⁴¹ In addition to escaping from predation, the formation of filamentous cells in some bacterial species, for instance *C. crescentus*, has been reported to acquire resistance to starvation, heat, oxidative stress, and changes in alkalinity.⁵ It is unclear if these stresses can induce morphological change in *C. crescentus*, but without the need of genetic modifications, the transformation into cell filamentation is a survival strategy adopted by *C. crescentus* to respond diverse environmental contexts. However, environmental shifts could be too dynamic for bacteria to attain a phenotype that senses and responds to certain environmental cues and thus to exhibit specific cell morphology. Instead, bacterial morphological plasticity might reflect its functional association with phenotypic heterogeneity in an isogenic population for coping with changing environments, in which genotypes can be allowed to persist but different phenotypic variants are manifested independently of environmental contexts.⁴² This is known as the *bet-hedging strategy* enabling some stressed subpopulations to gain adaptive benefits by increasing fluctuation levels in gene expression over time and between individual cells. Alternatively, the observation of opportunistic pathogen *Pseudomonas aeruginosa* during short-term growth in biofilm communities revealed extensive genetic diversification and phenotypic variation by a RecA-dependent mechanism.⁴³ This genetic diversity generally protects population from changing environmental contexts and is known as *insurance effect*. Though the principle of *insurance effect* is different from that of *bet-hedging strategy*, both strategies can cause phenotypic heterogeneity. Albeit phenotypic heterogeneity in the control of cell morphology may not directly associate with their morphological plasticity, the induction of morphological plasticity brings out the functional diversity derived from bacterial morphological changes in an isogenic population.

APPLICATIONS AND FUTURE WORKS

The molecular mechanism underlying the control of cell morphology has been suggested to be ultimately an epigenetic process in response to various physical constraints.¹⁹ Epigenetics, in a broad sense, describes cellular phenotypic variations caused by environmental factors that affect the transcription potential of genes without changing the underlying DNA sequence.⁴⁴ This consists with most observations of bacterial morphological plasticity in which induced morphological variants do not require alterations in genetic inheritances to undergo distinct developmental pathways toward morphogenesis for coping with changing environments and eventually revert to typical cell morphology in the absence of environmental adversity. However, research efforts about either genetic or epigenetic studies on bacterial morphological plasticity are hardly seen in previous investigations. This mostly ascribes to the fact that experimental models are lacking under laboratory operations and adequate tools are not available to dissect molecular mechanisms from sorted morphological variants. The recent discovery that *E. coli* can be mechanically induced into plethora morphological variants under the periodic micro-nanofluidic junctions¹⁷ (Figs. 6(a) and 4) could be a kick-start to investigate bacterial morphological plasticity under laboratory operations.

According to Waddington's perspective on epigenetic landscape, specific genetic mutations and reprogramming of key transcriptional factors might reshape the epigenetic landscape to regain pluripotency in differentiated stem cells.⁴⁴ L-form bacteria, or CWDB, induced by loss or defect of cell wall, are considered as the primitive progenitors of bacteria that are able to resume the cellular organization.¹¹ Therefore, it is intriguing if the epigenetic control of de novo generation of cell wall in CWDB could induce permanent morphological change without genetic manipulations. The bald conjecture is proposed here to stress the value of mechanically

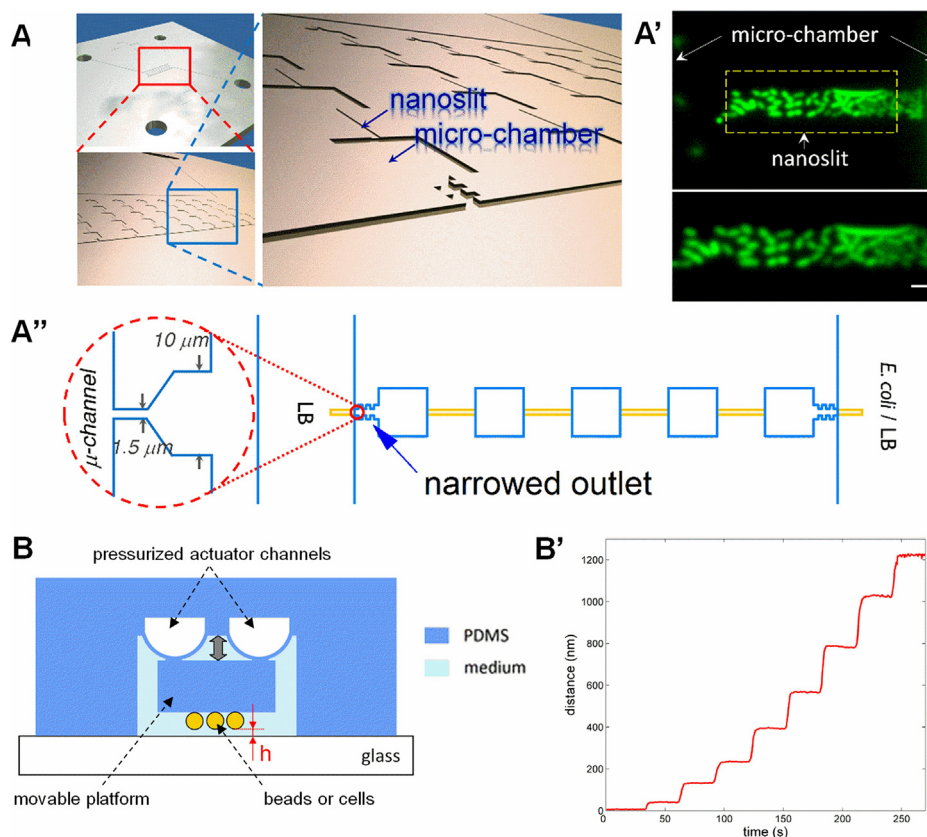


FIG. 6. Examples of micro-nanofluidic platforms for cell manipulations by periodic physical confinement (a-a'') and submicron control of channel height by pressure-actuated channels (b-b'). (A) Schematics of the microfluidic device used in this study with an H-shaped geometry (left upper inset), where repeated nanoslit ($L \times W \times H = 50 \times 10 \times 0.4 \mu\text{m}$)—micro-chamber ($L \times W \times H = 50 \times 50 \times 1.5 \mu\text{m}$) structures are bridged between two arms of the H-shaped microchannels (left lower inset and enlarged view in right inset). (a') Fluorescence images of *E. coli* penetrating a nanoslit (scale bar: $5 \mu\text{m}$). (a'') Top-view layout of an individual channel in (a) with close view of the outlet in the terminal microchamber (orange: nanoslits; blue: microchambers). Reprinted with permission from J. P. Shen and C. F. Chou, *Biomicrofluidics* **8**, 041103 (2014). Copyright 2014 AIP Publishing LLC. (b) Functional principle of submicron positional control in a PDMS-based biochip. The chip contains integrated actuators for positioning of the central PDMS platform carrying beads or cells. Then the central platform was approached to the glass surface by pressurizing the actuators. (b') The pressure–distance calibration curve. The distance between beads attached to the surface of the central platform and a glass slide was determined by reflection interference contrast microscopy as a function of the pressure. Before measurement, the pressure was increased till the bead touched the glass surface and defined as 0 mbar. Then, the pressure was reduced by 0.5 mbar every 30 s; the distance was measured in every 0.5 s. Reprinted with permission from R. Thuenauer *et al.*, *Lab Chip* **11**, 3064 (2011). Copyright 2011 Royal Society of Chemistry.

induced morphological variants under strong confinement. This model system can be performed under laboratory environment and the coupled micro-nanofluidic system potentiates the applications of genetic and epigenetic analysis in single-cell level. The possibility of permanent morphological change by physical or chemical means still requires great efforts to delve into the underlying molecular mechanisms of bacterial morphogenesis via epigenetic controls.

The requirement of microfluidic and nanofabrication technology

Apparently, several technologies are still needed to be implemented and integrated in the lab-on-a-chip platform to carry out the molecular dissections of complex morphological traits. First, microfluidic-based platforms exploiting different physical or chemical controls to manipulate bacterial morphologies are the essential tools to induce bacterial morphological plasticity. In addition to mechanical constraints as shown in Fig. 6(a), the generation of microenvironments in microfluidic devices to actuate graded changes of submicron channel height⁴⁵

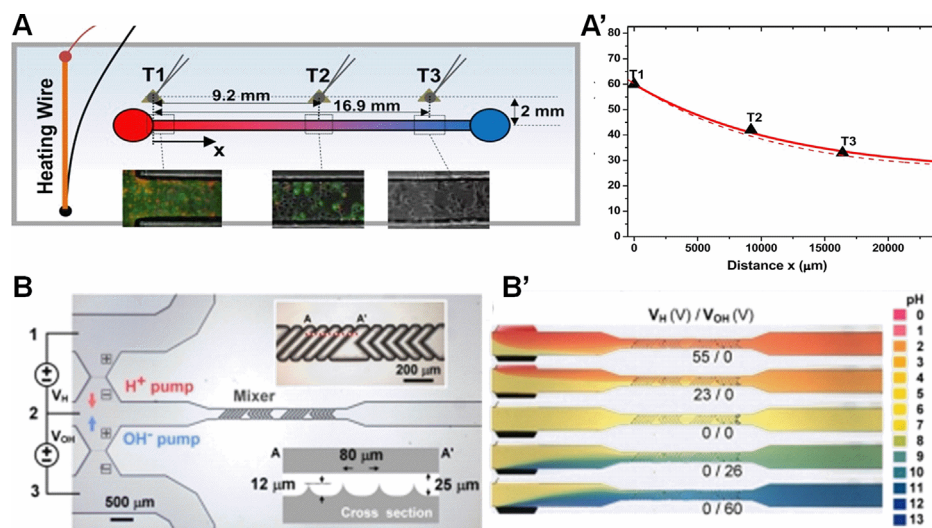


FIG. 7. Examples of microfluidic platforms for cell manipulations by the generation of temperature (a-a') and pH gradients (b-b'). (A) Schematic diagram (top view) of the microfluidic device integrated with a directional heating. The insets are the fluorescent images of cervix cancer cells on the first day post-heating located at the positions corresponding to each temperature measurement point T1-T3. (a') Temperatures T1-T3 were measured (solid line) and simulated (dot lines) along the microfluidics. Reprinted with permission from F. Wang *et al.*, *Biomicrofluidics* 6, 014120 (2012). Copyright 2012 AIP Publishing LLC. (b) Top view image of bipolar membrane-based microfluidic pH tuner. The pH adjustment is enabled by separately tuning the voltage biases across two upstream bipolar membranes, serving as proton and hydroxide ion pumps, via three Pt electrodes in the reservoirs. The numbers in the circuit indicate the corresponding electrodes in the reservoirs. The insets show the zoom-in image and the illustrated cross-section (not in scale) of the mixer channel. (b') Adjustment of voltage ratio V_H/V_{OH} determines pH gradients. Reprinted with permission from L. J. Cheng and H. C. Chang, *Biomicrofluidics* 5, 046502 (2011). Copyright 2011 AIP Publishing LLC.

(Fig. 6(b)) and establish the gradients of temperature⁴⁶ (Fig. 7(a)), reactive oxidative species,⁴⁷ or pH⁴⁸ (Fig. 7(b)) have been demonstrated to investigate cellular responses to parametric changes in these environmental factors. Similar designs could be integrated to provide the required environmental cues for induction of morphological plasticity under laboratory operations.

Next, sorting and isolation of morphological variants are critical for systematic investigations of bacterial morphological plasticity. Owing to diverse cell morphologies, microfluidic-based sorting/isolation approaches might require a combination of several mechanisms including gravity and hydrodynamic forces, dielectrophoretic, electrokinetic, magnetic, acoustic, laminar flow control, and microfiltering approach,⁴⁹ which have also been widely attempted to investigate stem cells in microfluidics. Unlike relative similar morphologies among stem cells, demanding in differentiation of wide-ranged cell size and shape diversity might challenge most sophisticated designs and fabrications to accomplish cell sorting and isolation for bacterial morphological variants.

Third, instead of using top-down approach to profile gene expression, the prior knowledge in bacterial morphogenesis and morphological plasticity enables a bottom-up approach to assemble all level information of biological pathways that coordinate morphological changes in contexts with environmental stresses.⁵⁰ To achieve this purpose, high-throughput single-cell RT-qPCR has been realized in a fully integrated microfluidic device for scalable analysis of gene expression in single cells.⁵¹ The molecular makers selected to reconstruct transcriptional network are based on the genes known for the modulation of PG assembly including the elongasome/divisome and auxiliary protein systems such as stress response/accessory envelop proteins.

Finally, to address the question about epigenetic reprogramming of bacterial morphological plasticity, the development of micro- and nanofluidic approaches could be very helpful in single-cell epigenetic profiling. For example, surface plasmon resonance biosensors have been coupled with microfluidic solid-state extraction system to enrich and characterize hyper-

methylated DNA from cancer cells.⁵² However, these approaches are still in technological infancy, and limited examples are available to demonstrate their practical applications in epigenetic studies,⁵³ thus marking their great potential and growth to tackle inherent epigenetic problems in single-cell level.

Taken together, the objective functions of microfluidic platform described here, in conjunction with genetic manipulation and strain selection, are the technological requirements to either clarify the role of distinct environmental cues in the long-term maintenance of specific morphological variants or to identify the molecular cues guiding bacterial morphological plasticity (Fig. 8).

A practical research strategy

Microfluidic approach has become a versatile tool in biological studies to aid generation of diverse microenvironments for supporting maintenance of plethora cellular phenotypes, and thus promoting insightful interrogations and dissections of the molecular mechanisms underlying distinct biological processes. While in the studies of bacterial morphological plasticity, multiple environmental factors and a multitude of strength levels in each cue span a broad parametric space and a daunting number of trial combinations. As six environmental cues suggested in Fig. 8 and 0 to 9 strength levels in each cue generate 10^6 theoretical combinations, extensive experimental efforts and extremely high cost incur an infeasible task to realize the searches of optimized parametric combinations. Likewise, the number of combinations could be even larger in orders of magnitude when expression of numerous biomolecules in genetic and epigenetic regulatory network is considered in response to the development of specific morphological variants. Apart from extensive labor, cost and time, sorting, and isolation of specific cell morphologies could be very challenging ascribing to vulnerable cell body of bacteria in context with deficient or defective cell wall. Unfortunately, the current knowledge is yet extremely limited to justify whether available microfluidic-based sorting/isolation methods⁴⁹ would introduce additional uncontrolled stresses that affect the development of distinct cell morphologies and the induction of morphological plasticity.

Alternatively, a research strategy to efficiently utilize available microfluidic technologies for the reduction of experimental efforts, rather than to invent new platforms with complicated designs and integrations, could also be a solution to overcome aforementioned difficulties and challenges. Recently, an efficient combinatorial drug screening method called the Feedback

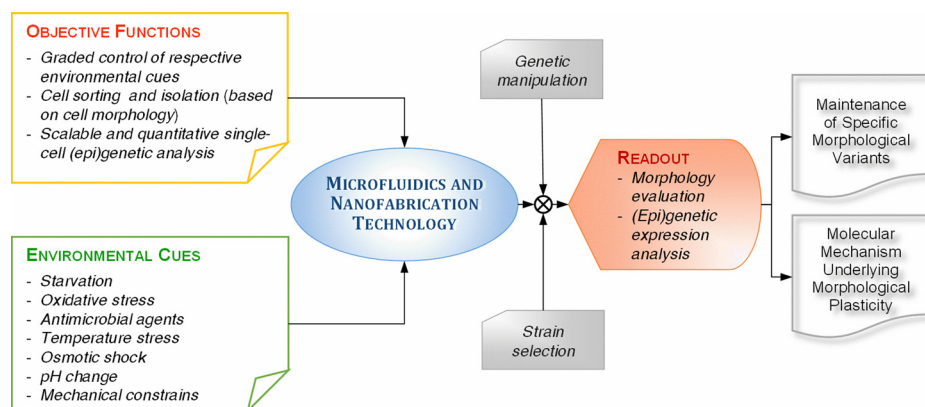


FIG. 8. Overview of the required technologies for the research of bacterial morphological plasticity. The joint merits of microfluidics and nanofabrication, genetic manipulation and strain selection form the technological basis to either support long-term maintenance of specific morphological variants or understand the molecular mechanism underlying morphological plasticity. To resolve these questions, sophisticated designs and integrations of different microfluidic technologies listed in the block of objective functions are required to induce and/or analyze morphological development in response to environmental cues listed in the figure. The readouts from microfluidic-based bioassays or experiments are subject to either morphological evaluation or genetic and/or epigenetic analysis to dissect molecular mechanism underlying bacterial morphological plasticity.

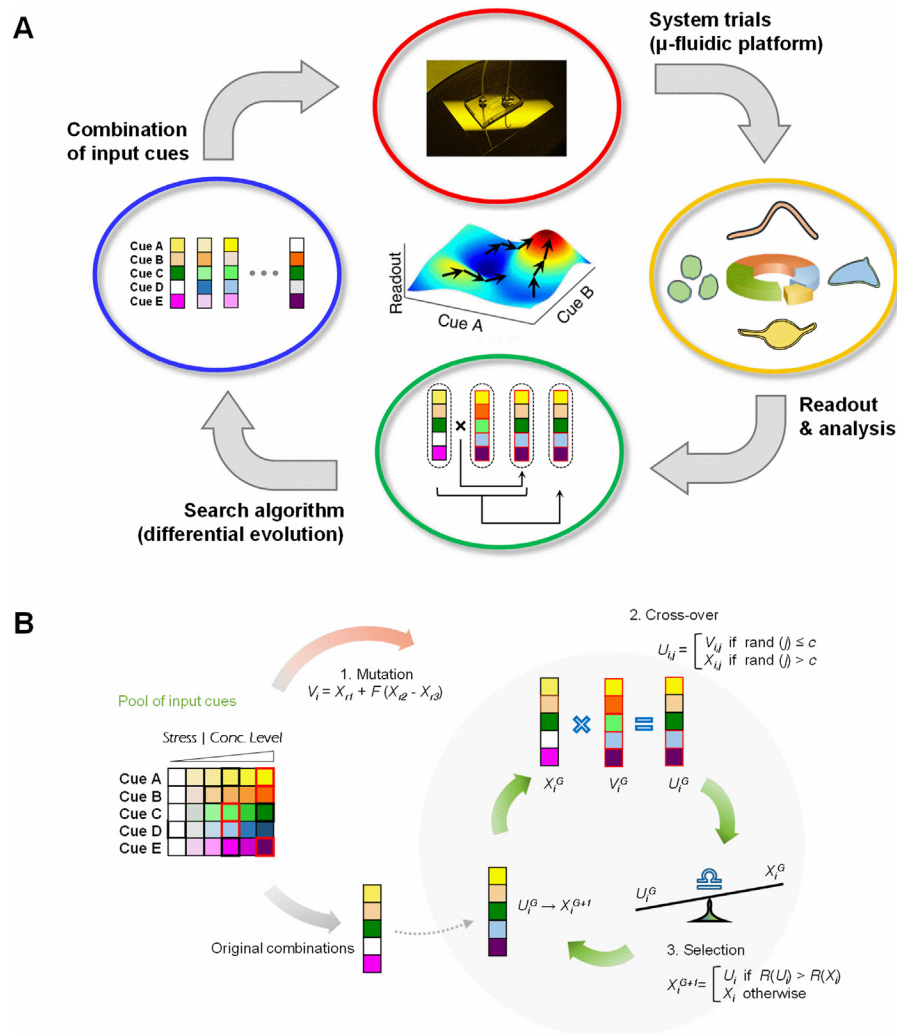


FIG. 9. Schematic diagrams of Feedback System Control (FSC) method (a) and Differential Evolution (DE) algorithm (b). (a) FSC method is formed by a closed-loop control of (1) combination of input cues, (2) system trials, (3) readouts, and (4) a stochastic search, or DE algorithm. FSC method combines bioassays and computational approach to iteratively optimize system output via DE algorithm for the generation of system input in the next iteration. (b) DE algorithm is a stochastic method and adopted in FSC method. In the first step, N (10-16) combinations of input cues are generated. For each original combination, a mutation (V_i) is generated based on the mathematical formula (step 1), where X_{r1-r3} are randomly selected from original combination. The parameter F represents how strongly the difference of the two randomly selected combinations is weighed during the mutation step. Then crossover combinations (U_i^G) are generated by crossing the originals and mutations, where random selection is performed based on comparing the values of a random number to the crossover constant C (step 2). The crossover combinations are subject to experimental trials for comparison of system outputs from crossover and original combinations (step 3). For those better outcomes from experimental comparison, new combinations (X_i^{G+1}) are generated and carried over to the next iteration. This series of processes is repeated until the desired phenotypic outputs are identified and achieved. Reprinted with permission from P. Nowak-Sliwinska *et al.*, Nat. Protoc. **11**, 302 (2016). Copyright 2016 Macmillan Ltd.

System Control (FSC) technique has been proposed^{54,55} to accomplish efficient combinatorial drug screening with orders of magnitude reduction in experimental efforts. Further, it also proved its valuable applications in an array of biological questions including the search of optimized conditions for the maintenance⁵⁶ and differentiation⁵⁷ of stem cells. FSC method follows an iterative process⁵⁵ (Fig. 9(a)) that integrates experimental results with a stochastic search guided by differential evolution (DE) algorithm (Fig. 9(b)) to seek a new combination as system input for the next iterative cycle until the optimized combination is attained. Such an optimization strategy does not require the prior knowledge about the pathway interactions elicited

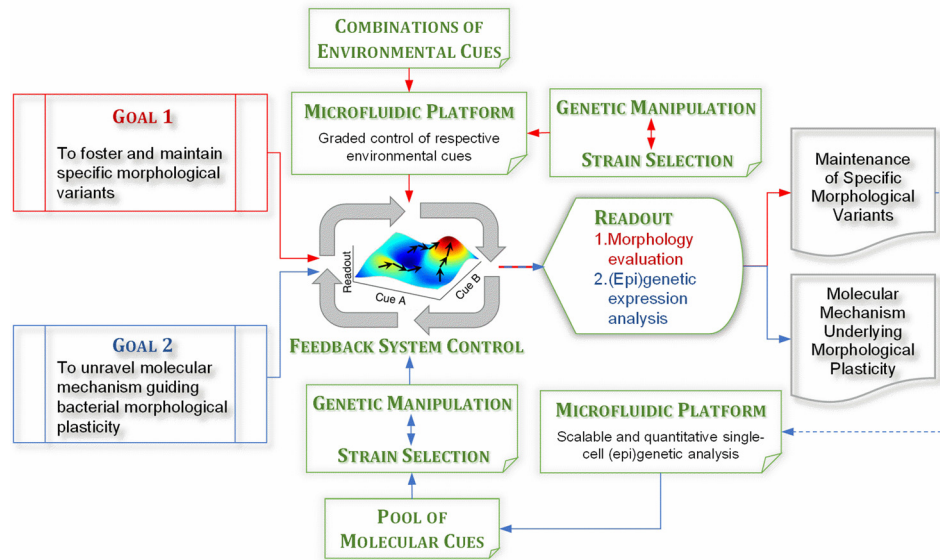


FIG. 10. Overview of practical research strategy for the studies of bacterial morphological plasticity. The closed-loop FSC method⁵³ combines microfluidic-based bioassays and a stochastic search algorithm to drive multi-level, multi-factor system toward optimized solutions and forms the kernel of proposed research strategy to reduce experimental labor, cost and time. Same questions raised to bacterial morphological plasticity as in Fig. 8 are stated in the blocks of goals 1 and 2. The strategy workflows (red arrow-line for goal 1 and blue arrow-line for goal 2) depict the requirement of technologies for resolving respective questions. Notably, combinations of environmental cues are the system inputs into FSC kernel; the pool of molecular cues selected from genetic and epigenetic analysis of the phenotypic outputs of goal 1 serves as the system inputs into FSC kernel.

by external stimuli, but it iteratively drives the system toward a desired phenotypic output by using the difference between the desired and the real system responses as optimization criteria in the search algorithm (Fig. 9(b)).

CWDB are described earlier to function as primitive progenitors of bacteria.¹¹ Therefore, the perspective of epigenetic landscape is thought to be applicable to CWDB as that does stem cells. Accordingly, two major questions are raised: (1) is it possible to support long-term maintenance of specific morphological variants without genetic modifications and (2) what are the molecular cues that enable the regulatory network guiding bacterial morphological plasticity? Though various microfluidic technologies are beneficial to resolve these questions, difficulties and challenges as mentioned earlier still prohibit insightful investigations, especially the underlying molecular basis and interplays. Instead, FSC technique could be the alternative that circumvents technological obstacles by transforming multi-level, multi-factor problems into the optimization of combinatorial cues. To bring the idea of FSC technique into practical solution, FSC method acts as a closed-loop platform by integrating microfluidic-based bioassay and a stochastic search kernel in a practical research strategy (Fig. 10). First, ascribing to microfluidic devices enabling graded control of respective environmental cues^{45–48} (Figs. 6(b), 7(a), and 7(b)), integration of multi-level, multi-factor controls in the system could elicit combinations of system inputs in FSC strategy, which is aimed to search optimized combinations of environmental cues that support long-term maintenance of specific morphological variants (goal 1 in Fig. 10). Notably, optimization criteria here could be evaluated by a search algorithm via statistical analysis of the difference between desired cell morphology and real cell morphologies. Apparently, once specific morphological variants were long-term maintained by FSC strategy, objective function of cell sorting and isolation in the microfluidic platform is no longer required thereby circumvents potential technical challenges. Next, combinations from a pool of molecular cues characterized by genetic and/or epigenetic profiling of specific morphological variant can serve as original combinations of system inputs. Following the FSC strategy (Goal 2 in Fig. 10), optimized combinations of selected key molecular cues could be identified for guiding bacterial morphological plasticity in stress-free environment, especially if the knowledge of

some key molecular cues is available. For example, the stress response/accessory envelope proteins are already known to be critical in *E. coli* on the developmental course of morphological reversion.¹³ By setting one of the optimization goals to maximize or minimize the dose of specific key molecule, the phenotypic outputs such as heterogeneous cell morphologies in population free from environmental stimuli may reveal the role of specific molecule in the control of bacterial morphological plasticity.

CONCLUSION

In a nutshell, the applications of microfluidics and nanofabrication technology to different biological systems have promoted profound understandings in biological questions from molecule to cell and systems levels and propelled the development of new methods and technologies to explore the new frontier where even challenging questions in different biological disciplines are undertaken. In particular, recent progresses exploiting microfluidic platforms to perform versatile researches on stem cell biology not only exemplify their powerful applications^{49,53} but also suggest similarly feasible and practical approaches under laboratory operations to probe, dissect, and unravel the molecular mechanisms underlying bacterial morphological plasticity. Here, micro-nanofluidic manipulations of bacteria have been shown to introduce strong perturbations upon bacterial morphogenesis network such that morphological plasticity can be induced via population heterogeneity in context with transcription potential of morphogenesis genes. How morphogenesis network is modulated or even rewired to induce bacterial morphological plasticity remains an open question. While strikingly, micro/nanofluidics-based approach could be the passkey to resolve all aspects of puzzles underlying bacterial morphological plasticity by exploiting FSC strategy to integrative microfluidic platform with a search algorithm that efficiently drives the system toward the desired output. Thereby, a practical research strategy is proposed in this review to support long-term maintenance of specific morphological variants and to identify optimized combinations of molecular cues guiding bacterial morphological plasticity.

ACKNOWLEDGMENTS

The authors thank Dr. Yi-Ren Chang for helpful discussions, Dr. Kerwyn Casey Huang and Yu-Ling Shih for providing bacteria strain imp4213 and plasmid pFX9, respectively, for some works involved here, and the technical support from Academia Sinica (AS) Nano Core Facilities. This work was supported in part by AS Nano Program, AS Thematic Projects (AS-103-TP-A01), Ministry of Science and Technology, Taiwan (102-2112-M-001-005-MY3, 103-2923-M-001-007-MY3), the Simons Foundation, and the hospitality of the Aspen Center for Physics (to C.-F.C.).

- ¹A. Typas, M. Banzhaf, C. A. Gross, and W. Vollmer, *Nat. Rev. Microbiol.* **10**, 123–136 (2012).
- ²K. D. Young, *Microbiol. Mol. Biol. Rev.* **70**, 660–703 (2006).
- ³K. D. Young, *Curr. Opin. Microbiol.* **10**, 596–600 (2007).
- ⁴S. S. Justice, D. A. Hunstad, L. Cegelski, and S. J. Hultgren, *Nat. Rev. Microbiol.* **6**, 162–168 (2008).
- ⁵M. A. Wortinger, E. M. Quardokus, and Y. V. Brun, *Mol. Microbiol.* **29**, 963–973 (1998).
- ⁶G. G. Anderson, J. J. Palermo, J. D. Schilling, R. Roth, J. Heuser, and S. J. Hultgren, *Science* **301**, 105–107 (2003).
- ⁷L. Dienes and H. J. Weinberger, *Bacteriol. Rev.* **15**, 245–288 (1951), available online at <http://www.ncbi.nlm.nih.gov/pmc/articles/PMC180721/#fn1>.
- ⁸W. A. Glover, Y. Yang, and Y. Zhang, *PLoS One* **4**, e7316 (2009).
- ⁹G. J. Domingue, Sr. and H. B. Woody, *Clin. Microbiol. Rev.* **10**, 320–344 (1997), available online at <http://www.ncbi.nlm.nih.gov/pmc/articles/PMC172922/>.
- ¹⁰R. Mercier, Y. Kawai, and J. Errington, *Cell* **152**, 997–1007 (2013).
- ¹¹J. Errington, *Open Biol.* **3**, 120143 (2013).
- ¹²D. S. Weiss, *J. Bacteriol.* **195**, 2449–2451 (2013).
- ¹³D. K. Ranjit and K. D. Young, *J. Bacteriol.* **195**, 2452–2462 (2013).
- ¹⁴R. Mercier, P. Dominguez-Cuevas, and J. Errington, *Cell Rep.* **1**, 417–423 (2012).
- ¹⁵J. Mannik, R. Driessen, P. Galajda, J. E. Keymer, and C. Dekker, *Proc. Natl. Acad. Sci. U. S. A.* **106**, 14861–14866 (2009).
- ¹⁶S. Takeuchi, W. R. DiLuzio, D. B. Weibel, and G. M. Whitesides, *Nano Lett.* **5**, 1819–1823 (2005).
- ¹⁷J. P. Shen and C. F. Chou, *Biomicrofluidics* **8**, 041103 (2014).
- ¹⁸J. L. Siefert and G. E. Fox, *Microbiology* **144**, 2803–2808 (1998).
- ¹⁹W. Margolin, *Curr. Biol.* **19**, R812–822 (2009).

- ²⁰C. Jiang, P. D. Caccamo, and Y. V. Brun, *Bioessays* **37**, 413–425 (2015).
- ²¹P. Szwedziak and J. Lowe, *Curr. Opin. Microbiol.* **16**, 745–751 (2013).
- ²²S. S. Justice, D. A. Hunstad, P. C. Seed, and S. J. Hultgren, *Proc. Natl. Acad. Sci. U. S. A.* **103**, 19884–19889 (2006).
- ²³A. Chauhan, M. V. Madiraju, M. Fol, H. Lofton, E. Maloney, R. Reynolds, and M. Rajagopalan, *J. Bacteriol.* **188**, 1856–1865 (2006).
- ²⁴R. R. Colwell and D. J. Grimes, *Nonculturable Microorganisms in the Environment* (ASM Press, 2000).
- ²⁵D. O. Serra, A. M. Richter, and R. Hengge, *J. Bacteriol.* **195**, 5540–5554 (2013).
- ²⁶S. Eriksson, S. Lucchini, A. Thompson, M. Rhen, and J. C. Hinton, *Mol. Microbiol.* **47**, 103–118 (2003).
- ²⁷D. S. Eto, J. L. Sundsbak, and M. A. Mulvey, *Cell Microbiol.* **8**, 704–717 (2006).
- ²⁸J. Pernthaler, *Nat. Rev. Microbiol.* **3**, 537–546 (2005).
- ²⁹G. Corno and K. Jurgens, *Appl. Environ. Microbiol.* **72**, 78–86 (2006).
- ³⁰R. D. Hayward, J. M. Leong, V. Koronakis, and K. G. Campellone, *Nat. Rev. Microbiol.* **4**, 358–370 (2006).
- ³¹M. A. Croxen and B. B. Finlay, *Nat. Rev. Microbiol.* **8**, 26–38 (2010).
- ³²J. M. Stevens, E. E. Galyov, and M. P. Stevens, *Nat. Rev. Microbiol.* **4**, 91–101 (2006).
- ³³O. Marches, V. Covarelli, S. Dahan, C. Cougoule, P. Bhatta, G. Frankel, and E. Caron, *Cell Microbiol.* **10**, 1104–1115 (2008).
- ³⁴D. A. Rosen, T. M. Hooton, W. E. Stamm, P. A. Humphrey, and S. J. Hultgren, *PLoS Med.* **4**, e329 (2007).
- ³⁵S. Bhatt, T. Romeo, and D. Kalman, *Trends Microbiol.* **19**, 217–224 (2011).
- ³⁶B. G. Spratt and K. D. Cromie, *Rev. Infect. Dis.* **10**, 699–711 (1988).
- ³⁷C. Miller, L. E. Thomsen, C. Gaggero, R. Mosseri, H. Ingmer, and S. N. Cohen, *Science* **305**, 1629–1631 (2004).
- ³⁸N. Markova, G. Slavchev, L. Michailova, and M. Jourdanova, *Int. J. Biol. Sci.* **6**, 303–315 (2010).
- ³⁹J. Errington, *Nat. Rev. Microbiol.* **13**, 241–248 (2015).
- ⁴⁰J. Dominguez-Escobar, A. Chastanet, A. H. Crevenna, V. Fromion, R. Wedlich-Soldner, and R. Carballido-Lopez, *Science* **333**, 225–228 (2011).
- ⁴¹P. N. Rather, *Environ. Microbiol.* **7**, 1065–1073 (2005).
- ⁴²M. Ackermann, *Nat. Rev. Microbiol.* **13**, 497–508 (2015).
- ⁴³B. R. Boles, M. Thoendel, and P. K. Singh, *Proc. Natl. Acad. Sci. U. S. A.* **101**, 16630–16635 (2004).
- ⁴⁴A. D. Goldberg, C. D. Allis, and E. Bernstein, *Cell* **128**, 635–638 (2007).
- ⁴⁵R. Thuenauer, K. Juhasz, R. Mayr, T. Fruhwirth, A.-M. Lipp, Z. Balogi, and A. Sonnleitner, *Lab Chip* **11**, 3064–3071 (2011).
- ⁴⁶F. Wang, Y. Li, L. Chen, D. Chen, X. Wu, and H. Wang, *Biomicrofluidics* **6**, 014120 (2012).
- ⁴⁷K. Y. Lo, Y. Zhu, H. F. Tsai, and Y. S. Sun, *Biomicrofluidics* **7**, 064108 (2013).
- ⁴⁸L. J. Cheng and H. C. Chang, *Biomicrofluidics* **5**, 046502 (2011).
- ⁴⁹H. W. Wu, C. C. Lin, and G. B. Lee, *Biomicrofluidics* **5**, 013401 (2011).
- ⁵⁰K. Shahzad and J. J. Loor, *Curr. Genomics* **13**, 379–394 (2012).
- ⁵¹A. K. White, M. VanInsberghe, O. I. Petriv, M. Hamidi, D. Sikorski, M. A. Marra, J. Piret, S. Aparicio, and C. L. Hansen, *Proc. Natl. Acad. Sci. U. S. A.* **108**, 13999–14004 (2011).
- ⁵²A. De, W. Sparreboom, A. van den Berg, and E. T. Carlen, *Biomicrofluidics* **8**, 054119 (2014).
- ⁵³T. Matsuoka, B. Choul Kim, C. Moraes, M. Han, and S. Takayama, *Biomicrofluidics* **7**, 041301 (2013).
- ⁵⁴P. K. Wong, F. Yu, A. Shahangian, G. Cheng, R. Sun, and C. M. Ho, *Proc. Natl. Acad. Sci. U. S. A.* **105**, 5105–5110 (2008).
- ⁵⁵P. Nowak-Sliwinska, A. Weiss, X. Ding, P. J. Dyson, H. van den Bergh, A. W. Griffioen, and C. M. Ho, *Nat. Protoc.* **11**, 302–315 (2016).
- ⁵⁶H. Tsutsui, B. Valamehr, A. Hindoyan, R. Qiao, X. Ding, S. Guo, O. N. Witte, X. Liu, C. M. Ho, and H. Wu, *Nat. Commun.* **2**, 167 (2011).
- ⁵⁷Y. Honda, X. Ding, F. Mussano, A. Wiberg, C. M. Ho, and I. Nishimura, *Sci. Rep.* **3**, 3420 (2013).